scientific reports

Check for updates

OPEN

Impact of virgin and recycled polymer fibers on the rheological properties of cemented paste backfill

Zhuoqun Yu[1]✉, Wenjun Kong[1], Zhiqiang Ji[1] & Yongyan Wang[2]

The addition of polymer fibers to cemented paste backfill (CPB) has shown promise in enhancing mechanical properties, although it also introduces changes in rheological characteristics. This study aimed to investigate the influence of different types of polymer fibers, namely virgin commercial polypropylene fiber (CPPF), recycled tire polymer fiber (RTPF), and recycled tire rubber fiber (RF), on the rheological properties of CPB mixtures through an experimental program, and provide design references for CPB pipeline transport. The results revealed consistent reductions in bulk density upon the incorporation of polymer fibers into CPB, alongside varying impacts on slump. Specifically, the addition of CPPF had a mild effect, while RTPF caused a continuous decrease in slump, and RF exhibited minimal influence up to a 4% concentration, with substantial effects thereafter. Moreover, the inclusion of fibers led to increases in apparent viscosity parameters, with RTPF inducing the most significant changes, followed by varying responses from CPPF and RF. When using RTPF for CPB reinforcement, emphasis should be placed on enhancing technical indicators related to viscosity such as energy consumption and pipeline wear during pipeline transport. Furthermore, adjustments were necessary to account for flow curve instability resulting from interactions between fibers and the paddle, with the data aligning well with the Bingham model. The addition of fibers, particularly CPPF and RF, primarily influenced plastic viscosity rather than yield stress, underscoring the limitations of slump tests in assessing rheology.

Keywords Recycled materials, Polymer fibers, Waste tire, Tailings

The extraction of minerals is accompanied by the formation of underground voids and the generation of solid waste predominantly in the form of tailings. These factors have the potential to cause severe environmental problems. Gradually, the cemented paste backfill (CPB) technology has become an increasingly prominent practice to improve the stability of underground voids, improve mine safety, and to provide a safe management approach for the tailings with lower ecological consequences[1–3]. Typical CPB is the mixture of tailings, cement (3% to 10% by dry mass of tailings) and water, which solid content is often between 70 and 85%[4–6]. After being mixed at the backfill station, the fresh CPB mixture will be transported into underground voids through a pipeline system and left to cure until it reaches a target strength.

The delivery of CPB plays a vital role in ensuring the effectiveness and reliability of CPB technology in various applications. Recently, the emergence of long-distance deep-sea mining and deep-depth mining[7–9] with more intricate pipeline designs underscores the necessity for more comprehensive investigation into the rheological properties of CPB. Rheological parameters of CPB, such as yield shear stress and viscosity, should be determined for characterizing its flow behavior as a guidance. The yield shear stress represents the minimum pressure required to initiate flow. A lower yield shear stress could facilitate the selection of a more cost-effective and energy-efficient pumping method[10]. Viscosity represents the frictional force between two layers of fluid, which affects the pressure head loss during the flow. Considering the significance of these rheological parameters for the CPB delivery, numerously experimental studies have been conducted. Results have shown that the temperature, mixing intensity, solid content, and specific substances are among the factors that can influence the CPB rheological properties[11–14]. For example, Ouattara et al.[15] demonstrated that superplasticizers have the capacity to decrease the yield stress and plastic viscosity of CPB. This reduction is significantly influenced by factors such

[1]Yantai University, Qiangquan Road No.30, Yantai, China. [2]Qingdao University of Science and Technology, Songling Road No.99, Qingdao, China. ✉email: yzqun2007@126.com

as the solid content of CPB, the type of binder employed, and the specific type of superplasticizer being used. Yan et al.[16] found that the hydrophobic agent mainly affects the shear stress of CPB under a shear rate of 50 s^{-1}. Xiao et al.[17] reported that increasing the slag content in slag-CPB leads to decreased flowability, which could elevate the risk of pipeline blockages during transportation. Moreover, the introduction of superabsorbent polymers[18] and superplasticizer[19] have obvious impact in the yield stress and viscosity of the CPB mixture. In light of this, it is important to approach with caution and conduct thorough analysis when introducing any new materials into CPB, as they have the potential to cause significant changes in its rheological characteristics.

As cement usage contributes to environmental impacts and accounts for approximately 70% of backfill cost, researchers have conducted extensive studies to explore approaches of enhancing the mechanical performance while limiting cement dosage[20]. Alongside the utilization of innovative environmentally sustainable bonding agents as a substitute for cement, the introduction of fibers into CPB has been identified as a feasible technique[21–24]. It has previously been observed that the inclusion of virgin fibers such as polypropylene fiber, glass fiber, and polyacrylonitrile fiber improved the stiffness and ductility of CPB and reduced the cement cost[25,26]. However, the inclusion of virgin fibers has shown limited effectiveness in cost reduction and pollution mitigation. Therefore, researches on incorporating recycled fibers such as rice straw, rubber fiber, and tire polymer fiber into CPB have been conducted[27–29]. Results have shown that the inclusion of an appropriate amount of recycled fibers had a positive effect on certain mechanical performance aspects of CPB, as well as better economic and environmental gains.

The flow behavior of CPB incorporating fibers is typically evaluated by slump tests, which provide a range of values to demonstrate its workability. Nevertheless, the slump test result is associated with low accuracy and only partially reflects the rheological properties of the material, which may result in a less precise approach to pipeline transportation design. Despite a few researchers have conducted studies on the rheological properties of CPB incorporating with polymer fibers using both slump and rheometer tests, the fibers used have consistently been virgin commercial fibers, primarily polypropylene fibers[30,31]. Virgin polymer fibers refer to fibers that are made from new, unused polymer materials without any prior use or processing. These fibers have not been previously incorporated into any product or undergone any recycling process. On contrary, recycled polymer fibers are fibers that are produced from polymer materials that have been used in products, discarded, and then processed to be reused. The intricate chemical composition and unique physical characteristics of recycled fibers result in an interaction mechanism with multiple factors influencing rheological properties of CPB. Consequently, the effect of recycled fibers on the flow behavior of CPB is complex and unclear. Up to now, there is currently a lack of comprehensive rheological studies on CPB incorporating recycled polymer fibers.

Hence, this paper investigates the rheological properties of CPB incorporating two recycled polymer fibers derived from scrap tires, namely recycled tire polymer fiber (RTPF) and recycled tire rubber fiber (RF), which have already been testified to positively impact the mechanical behavior of CPB and contribute to mitigate the black pollution caused by scrap tires[28,29]. Additionally, CPB incorporated with (CPPF) is investigated for comparison and to aid in mechanism analysis of recycled polymer fibers effects. Both slump tests and rheometer tests were conducted for this purpose. The research findings will serve as scientific references for a more precise evaluation of the rheological behavior of recycled polymer fiber-reinforced CPB and for assessing the consistency between slump tests and rheometer tests. This will facilitate the engineering application of recycled polymer fiber additives in CPB.

Materials and methods

The overall flowchart depicting the characterization of materials and testing procedures in this study is illustrated in Fig. 1.

Materials

Tailings

The tailings applied in this study was obtained from an iron mine in the southern Shandong, China. A laser particle size analyzer (Mastersizer 2000, Malvern) was used to analyze the particle size distribution. The particle size distribution of the tailings is presented in Fig. 2. The main chemical compositions obtained from X-ray fluorescence and physical properties of the tailings are shown in Table 1.

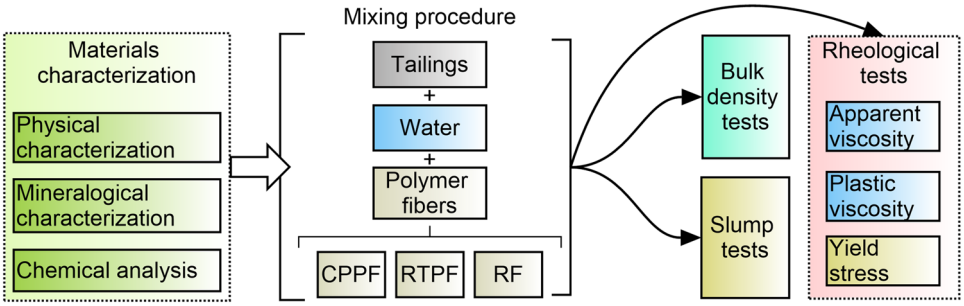

Figure 1. Flowchart of the materials characterization and testing procedures.

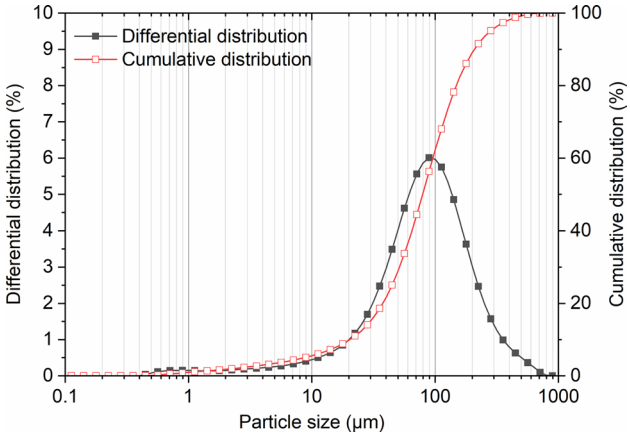

Figure 2. Particle size distribution of the tailings.

Chemical composition (%)	Tailings	Physical properties	Tailings
SiO_2	55.50	Specific gravity	2.76
Al_2O_3	2.93	Specific surface (cm^2/g)	2640
Fe_2O_3	23.80	D_{10} (μm)	20.41
MgO	3.18	D_{50} (μm)	79.62
CaO	5.26	D_{90} (μm)	208.89
SO_3	0.41		
Na_2O	0.62		
K_2O	0.80		
P_2O_5	0.38		
MnO	0.21		
TiO_2	0.12		

Table 1. Main chemical and physical properties of tailings and cement used in this study.

Binder

The ordinary portland cement (P.O. 42.5) was utilized as the binder. The main chemical and physical properties of the cement are shown in Table 2. The most common cement dosage in CPB is between 3 and 10% by the weight of the tailings[6,32,33]. The main focus of this paper is to investigate the influence of fibers on CPB rheological properties. Therefore, the cement content in this study was chosen to be constantly 5% by dry tailings weight based on the experience from the backfill plant and published literatures[34].

Fibers

The main characteristics of the polymer fibers utilized in this study are summarized in Table 3. As shown in Fig. 3a, the RTPFs used in this study pertains to polymer fiber fluff, which is a residual substance resulting from the grinding process of scrap tires. The RTPF primarily comprises polyester fibers, meanwhile it may unavoidably contain traces of rubber ash. The average length and diameter of RTPFs were 9.0 mm and 0.03 mm, respectively. The morphological characteristics of the RTPFs, as illustrated in Fig. 3b, demonstrates their twisted and intertwined structure, accompanied by the presence of residual rubber particles on the surface. By comparison, the CPPF as illustrated in Fig. 3c employed in this study is a commercially available virgin material. The average length and width of the CPPFs were 6.0 mm and 0.1 mm, respectively. In accordance with the accumulated experience from prior studies on micro fiber (equivalent diameter less than 0.3 mm) usage in cement-based materials[6,23,35], the RTPF and CPPF contents used in this investigation were determined as 0%, 0.3%, 0.6%, and 0.9% by dry solids weight. Based on field investigations and prior literature, the RTPF to CPPF price ratio was approximately 1:1.8, leading to reduced material costs and enhanced mechanical properties.

Chemical composition	SiO_2	Al_2O_3	Fe_2O_3	MgO	CaO	SO_3
Content (%)	21.4	4.31	4.91	3.00	62.34	2.20

Table 2. Main chemical composition of the cement used in this study.

Physical properties	RTPF	CPPF	RF	Other features	RTPF	CPPF	RF
Specific gravity	0.96	0.91	1.09	Major ingredient	Polyester	Poly-propylene	Rubber
Average length (mm)	10.0	6.0	16.0	Impurity	Rubber	None	None
Average diameter (mm)	0.03	0.1	2.0				
Water absorption (%)	> 0.4	< 0.03	> 1.0				
Tensile strength (MPa)	620	590	26.2				

Table 3. The main characteristics of the RTPF and CPPF.

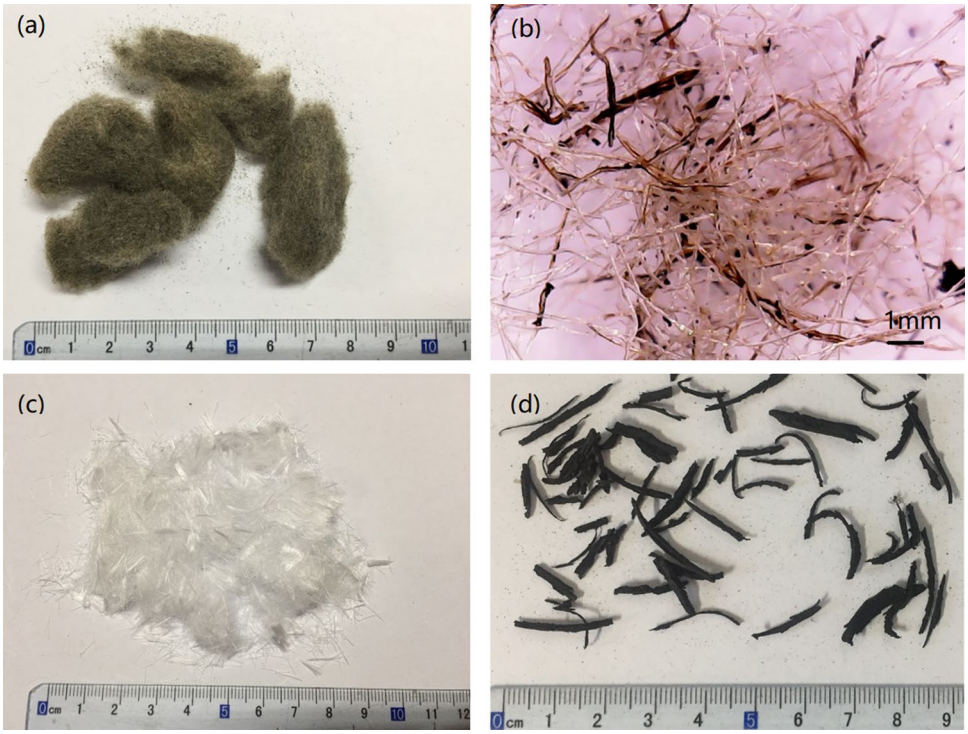

Figure 3. Pictorial view of the (**a**) RTPF, (**b**) RTPF at 10 × magnification, (**c**) CPPF, and (**d**) RF.

RFs employed in this study were obtained from the mechanical shredding of the scrap tires. The average length and width of the rubber fibers were 16.0 mm and 2.0 mm, respectively. Based on the dosage of recycled macro fibers (equivalent diameter larger than 0.3 mm) for cement-based materials reported in existing literature[28,36], the RF contents in this study were selected as 0%, 2%, 4%, and 6% by weight of the dry solids. It is acknowledged that rubber fibers cost approximately $250 per ton in China. Nevertheless, since the modified CPB will utilize substantial quantities of scrap tires, the environmental advantages it offers will outweigh its economic expenses. In the future, mining enterprises may no longer need to purchase tires as raw materials, but instead, they could offer scrap tire disposal services as part of their pollution abatement efforts.

Methods

Preparation of CPB mixtures

CPB mixtures were prepared with varying contents of RTPFs, CPPFs, and RFs. Based on the common binder dosage of CPB in the mine site, the binder content and solid content of the mixtures were determined to be 5% and 75% respectively. Table 4 presents the proportion design of CPB mixtures in this study. To ensure precise preparation of CPB mixtures, the materials were weighed using an electric scale with an accuracy of 0.01 g. The dry tailings, along with specific amounts of cement and tap water, were initially mixed in a laboratory mixer, followed by the addition of pre-weighed RTPFs, CPPFs, or RFs. The mixing time for all mixtures was maintained at a constant duration of 15 min. This study focuses on investigating the influence of different fibers on the rheological properties of CPB mixtures. Therefore, the effect of varying curing times on the rheological properties of CPB is not considered at this stage. Once the CPB mixtures are prepared, testing is conducted immediately. It is noted that reports of mechanical properties of cured CPB corresponding to all proportions in this study can be found in previous researches[28,29], which is of practical significance for engineering applications.

No	Fiber type	Fiber content	Cement content (%)	Solid content (%)
1	–	0.0%	5	75
2–4	RTPF	0.3%/0.6%/0.9%	5	75
5–7	CPPF	0.3%/0.6%/0.9%	5	75
8–10	RF	2.0%/4.0%/6.0%	5	75

Table 4. Proportion design of CPB mixtures in this study.

Bulk density measurements on CPB mixtures

Bulk density of each CPB mixture as listed in Table 3 was measured using a density cup methodology. During the test, the temperature was maintained at 20 ± 0.5 ℃, the pre-mixed CPB mixture was carefully poured into the calibrated density cup, avoiding the formation of bubbles or spillage. The external surface and rim of the density cup were meticulously cleaned. After positioning the density cup containing the sample on the electric scale, the mass was recorded. Bulk density was calculated using the mass and volume measurements based on the ASTM D7263-09. To enhance precision, duplicated measurements were performed, and the average value was calculated.

Rheological tests on CPB mixtures

Figure 4 shows the rheological tests in this study. The slump test was conducted to estimate the rheological properties of CPB. Drawing upon the fundamental principles outlined in ASTM C 143 for the standard slump test[37], the cylinder slump test was chosen as the preferred method due to the limited availability of materials for laboratory testing. The small cylinder with 110 mm diameter and 110 mm height was used[38].

The rheological properties was tested using a rotational rheometer (Brookfield, Middleborough, USA) with a vane geometry of 15 mm diameter and 30 mm height. On the basis of shear deformation theory and non-Newtonian fluid theory, experimental methods aimed at characterizing the rheological properties of CPB slurry were designed. During the test, the temperature was maintained at 20 ± 0.5 ℃, the pre-mixed CPB mixture was poured into the rheometer container, and after removing air bubbles through vibration, it was slowly pressed with the rotor to ensure complete immersion of the vane in the mixture while maintaining a distance of at least 20 mm from the bottom and top of the mixture. The Rheo3000 software was utilized for programming, setting the rheological shear program to control shear rate mode. Over a period of 120 s, the shear rate linearly increased from 0 to 120 s^{-1}, followed by a 1-s reduction back to 0 s^{-1}. Data were recorded in terms of dynamic viscosity curves and flow curves.

Average apparent viscosity was calculated based on the dynamic viscosity curves. In addition, the cross model as described in Eq. (1) was used to fit the viscosity curves to obtain the infinite dynamic shear viscosity.

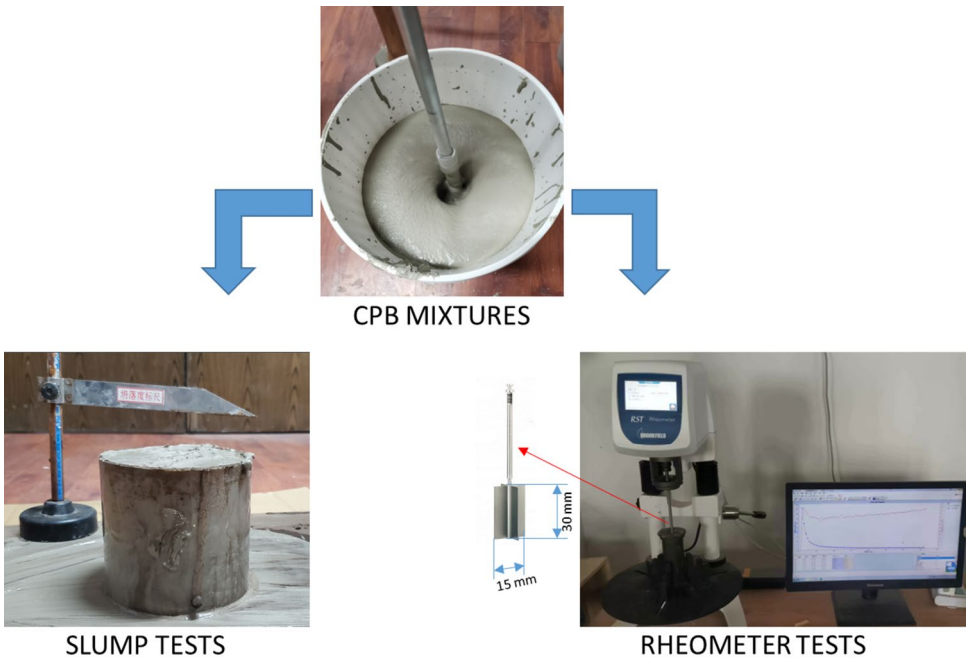

Figure 4. Diagram of the rheological properties tests for CPB mixtures.

$$\mu = \mu_\infty + \frac{\mu_0 - \mu_\infty}{[1 + (C\gamma)^n]} \quad (1)$$

where μ_0 and μ_∞ are the initial shear viscosity (Pa·s) and infinite shear viscosity (Pa·s), respectively, C is the cross consistency index, γ is the shear rate (s^{-1}), n is the Cross shear flow index. The infinite shear viscosity is a parameter that indicates the viscosity reached by the dynamic viscosity curve at higher shear rates ($\geq 100\ s^{-1}$).

The Bingham model which is often used to describe the rheological behavior of the non-Newtonian materials, was used to characterize the CPB flow curves in this study, as expressed in Eq. (2).

$$\tau = \tau_0 + \mu_c \gamma \quad (2)$$

where τ is the shear stress (Pa), τ_0 is the yield stress (Pa), μ_c is the plastic viscosity (Pa·s), γ is the shear rate (s^{-1}). In accordance with the Bingham model, if the shear stress exerted on the CPB mixture is below the yield shear stress, the mixture will not undergo any deformation. However, once the applied shear stress surpasses the yield shear stress, the mixture exhibits Newtonian flow behavior, where the shear stress shows a linear relationship with the shear rate.

Results and analysis

Effect of fibers on the bulk density and slump values of CPB mixtures

Figure 5 illustrates the variation in bulk density for CPB mixtures. It can be observed that the bulk density decreases as the fibers content increases for all three types of fibers investigated in this study. The bulk density of CPB without any fibers decreases by 0.57%, 0.55% and 3.28% after the inclusion of 0.9% of CPPF, 0.9% of RTPF, and 6% of RF, respectively. The main reason for the decrease in bulk density is the lower density of polymer fibers compared to tailings.

The slump test results for CPB mixtures are presented in Fig. 6. As shown in Fig. 6a, the slump values of the CPPF-modified CPB mixtures exhibit no significant change as the CPPF content increases. However, it is evident that the slump values of the RTPF-modified CPB mixtures gradually decrease with an increase in RTPF content. The contrasting variations in slump values between the two types of polymer fibers can primarily be attributed to the higher water absorption rate of RTPF than the CPPF. Additionally, the impurity in RTPFs, specifically rubber ash, exhibit an extremely fine particle size and relatively higher specific surface area (than polymer fibers), resulting in enhanced capture of free water and reduced flowability. Moreover, the entangled and twisted structure of the RTPFs can easily form a three-dimensional network, which assists in maintaining the shape of the CPB mixture during the slump test and consequently yields lower slump values. Furthermore, Fig. 6b demonstrates that the slump value of RF-modified CPB mixtures initially slightly decreases with an increase in RF content until a significant decrease is observed at 6% content. This phenomenon can be explained by the physical properties of RF. As indicated in Table 3, RF has a coarser filament diameter compared to polymer fibers, leading to diminished free water capture capability. Consequently, within the range of 2% to 4% RF content, the slump value of the RF-modified CPB mixtures exhibits little variation. In addition, with a continuous increase in RF content, at the 6% threshold, the probability of contact between rubber filaments within the mixture dramatically rises, resulting in increased friction and a subsequently reduced slump value of the CPB mixture.

Ordinary CPB often exhibits high consistency in terms of slump and bulk density[38]. However, upon observing Figs. 5 and 6, it becomes evident that the consistency is disrupted when polymer fibers are added into CPB mixtures.

Effect of fibers on the viscosity of CPB mixtures

Numerous studies have indicated that CPB mixtures behave as non-Newtonian fluids[39]. The viscosity of non-Newtonian fluids is not constant, it varies with the rate of shear, resulting in different viscosities at different

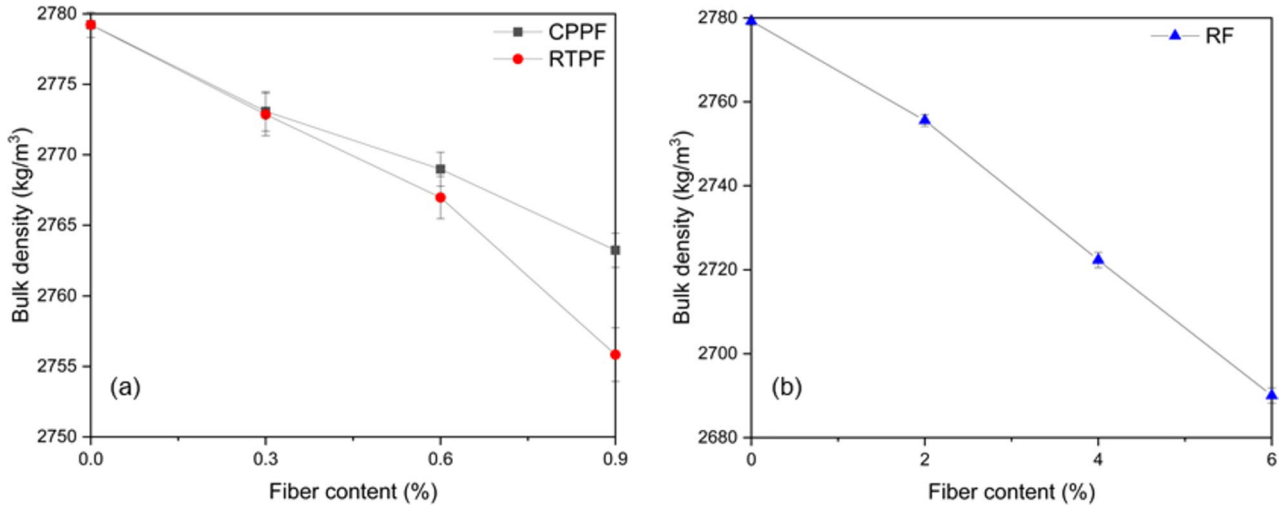

Figure 5. Bulk density of CPB mixtures containing (**a**) CPPF, RTPF, and (**b**) RF.

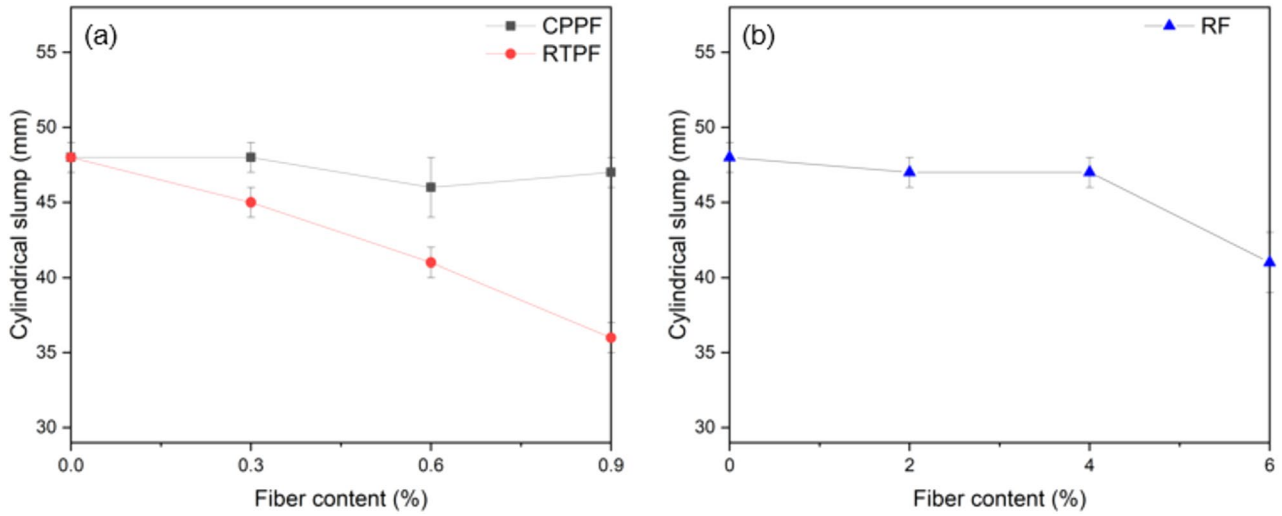

Figure 6. Slump tests results of CPB mixtures containing (**a**) CPPF, RTPF, and (**b**) RF.

shear rates. Consequently, the viscosity at a specific shear rate is defined as the apparent viscosity, which reflects the flowability of the fluid at that shear rate. Experimental data obtained from the rheometer are compiled as shown in Fig. 7. Since the CPB slurries maintain constant cement content and solid mass concentration, different curves are distinguished by modified material types and their proportions. Preliminary observation from the Fig. 7 reveals that at low shear rates (less than 10 s^{-1}), the apparent viscosity is relatively high, while at shear rates exceeding 10 s^{-1}, viscosity continuously decreases and stabilizes. This phenomenon is attributed to the presence of fine particles in the CPB mixture during static conditions and the relatively high solid concentration, whereby the electrostatic field on the particle surfaces induces strong flocculation, forming an internal flocculation network structure within the CPB mixture. Consequently, during the initial stages of shear, the flocculation network structure within the CPB mixture endows it with a higher apparent viscosity. However, the network structure induced by the CPB mixture particle flocculation is susceptible to shear forces. With the sustained increase in shear rate, the flocculation network structure is stretched, breaking down into flocculation clusters, and ultimately dispersing into smaller particles, resulting in a corresponding gradual decrease in apparent viscosity. Moreover, as flocculation induced by the particles persists, at high shear rates, there is an increased chance of collision and contact among particles within the mixture, leading to a dynamic equilibrium between the destruction and repair of the mixture's internal structure, thereby stabilizing the apparent viscosity. Furthermore, it is observed from Fig. 7 that at the same shear rate, the apparent viscosity of CPB with fibers is higher than that of conventional CPB. This is attributed to the added materials acting as fiber-like entities, intertwining and overlapping within the mixture to form a fibrous network structure. These fibrous network structures further reinforce the internal structure of the CPB mixture in conjunction with the flocculation network structure of the tailings particles, resulting in increased fluid flow resistance and higher apparent viscosity. Similarly, with the increase in shear rate, the network structure of the fibers is also disrupted, dispersing into smaller network structures or even single fibers, leading to a decrease in apparent viscosity.

As shown in Fig. 8, the average apparent viscosity of CPB incorporated with CPPF is slightly higher compared to that of the conventional CPB. An increase in the content of CPPF leads to a slight increase in the average apparent viscosity of the CPB mixture, with a doubling observed when the content of CPPF reaches 0.9% compared to the conventional CPB. The average apparent viscosity of the CPB incorporated with RTPF is much higher compared to that of the conventional CPB. It reaches its maximum at a RTPF content of 0.6%, with the average apparent viscosity being 6.1 times higher than that of the conventional CPB. As the content of RTPF continues

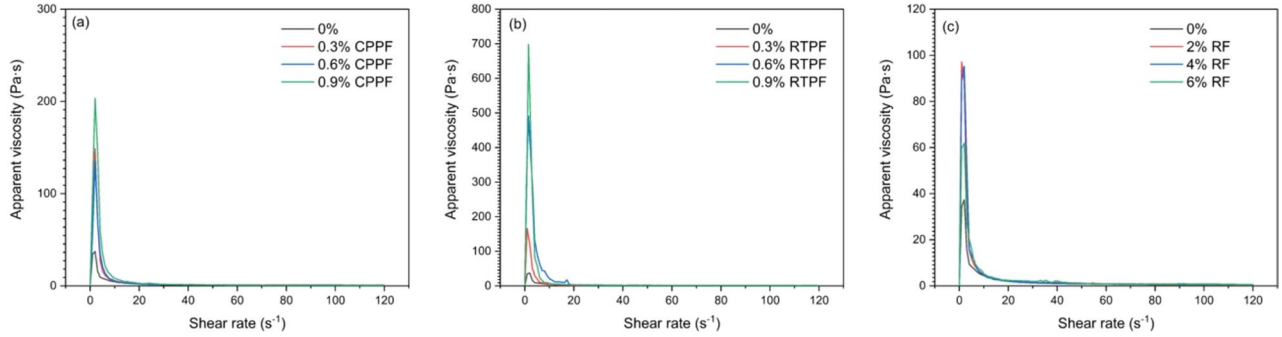

Figure 7. Apparent viscosity curves of CPB incorporated with (**a**) CPPF, (**b**) RTPF, and (**c**) RF.

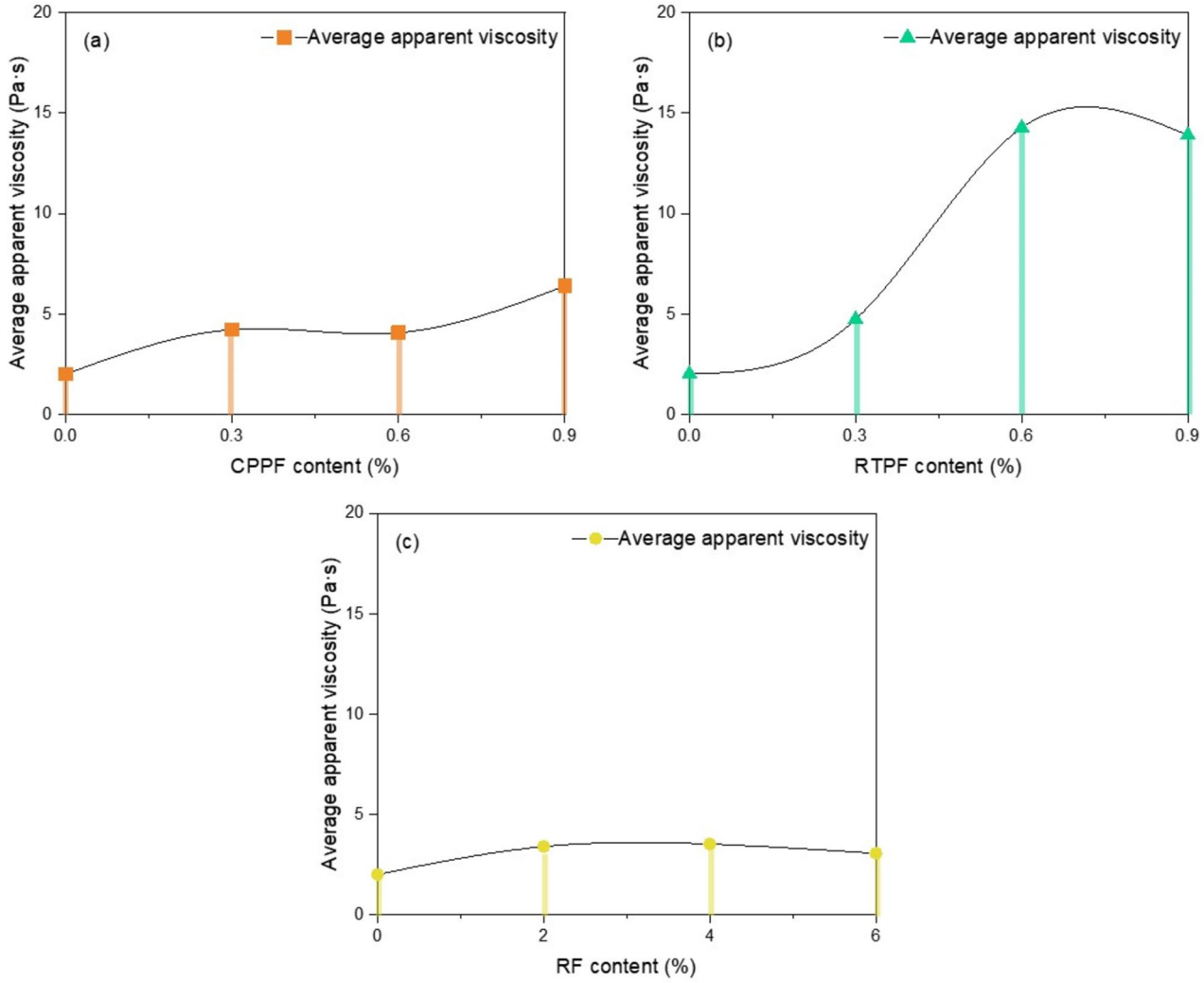

Figure 8. Average apparent viscosity of CPB incorporated with (**a**) CPPF, (**b**) RTPF, and (**c**) RF.

to increase to 0.9%, the average apparent viscosity slightly decreases. Unlike CPPF and RTPF, the increase in the content of RF does not significantly elevate the average apparent viscosity of the CPB.

Figure 9 illustrates the impact of polymer fibers on the infinite viscosities of CPB. As depicted in Fig. 9a, the rise of CPPF content in CPB exhibits a zigzagging upward trend in infinite viscosity, akin to the pattern observed in average apparent viscosity. Conversely, Fig. 9b portrays a consistent increase in infinite viscosity with the escalation of RTPF content in CPB, deviating from the trend curve of average apparent viscosity. The impact of RF content on the ultimate viscosity is very slight as shown in Fig. 9c, which is similar to its effect on the average viscosity. Due to the high shear rates existing on the pipeline wall during the CPB transport, the infinite viscosity is considered a reliable supplementary parameter for assessing the rheological behavior of materials during transport[18,40]. The discrepancy between the average apparent viscosity and the infinite viscosity of RTPF-modified CPB suggests a significant difference in viscosity at high shear rates compared to low shear rates, indicating that the viscosity of RTPF-modified CPB varies considerably with RTPF content at high shear rates compared to low shear rates.

Effect of fibers on the flow curves of CPB mixtures

The flow curves for both types of CPB mixtures containing various of polymer fibers are presents in Fig. 10. It can be observed that when the shear rate starts increasing from 0 s^{-1}, the shear stress sharply increases within a few seconds, reaching a high peak. This phenomenon is known as stress overshoot. The primary reason for this phenomenon is that when the rheometer motor starts and drives the rotor to rotate, it needs to overcome the yield stress of the mixture to induce shear flow. However, there is a lag in this process, resulting in an extremely high peak stress[41]. The presence of stress overshoot indicates the presence of a strong network-like structure with relatively high strength within the CPB mixture. For CPB containing fibers, the peak of the stress overshoot is significantly higher than that of the CPB without fibers. As the shear rate continues to increase, the shear stress decreases and tends to stabilize. Additionaly, it can be observed that the flow curves of CPB mixtures containing fibers exhibit notable fluctuations, particularly at higher levels of fiber content. These fluctuations occur due to the detection of torque spikes by the rheometer when the blades come into contact with the fibers during

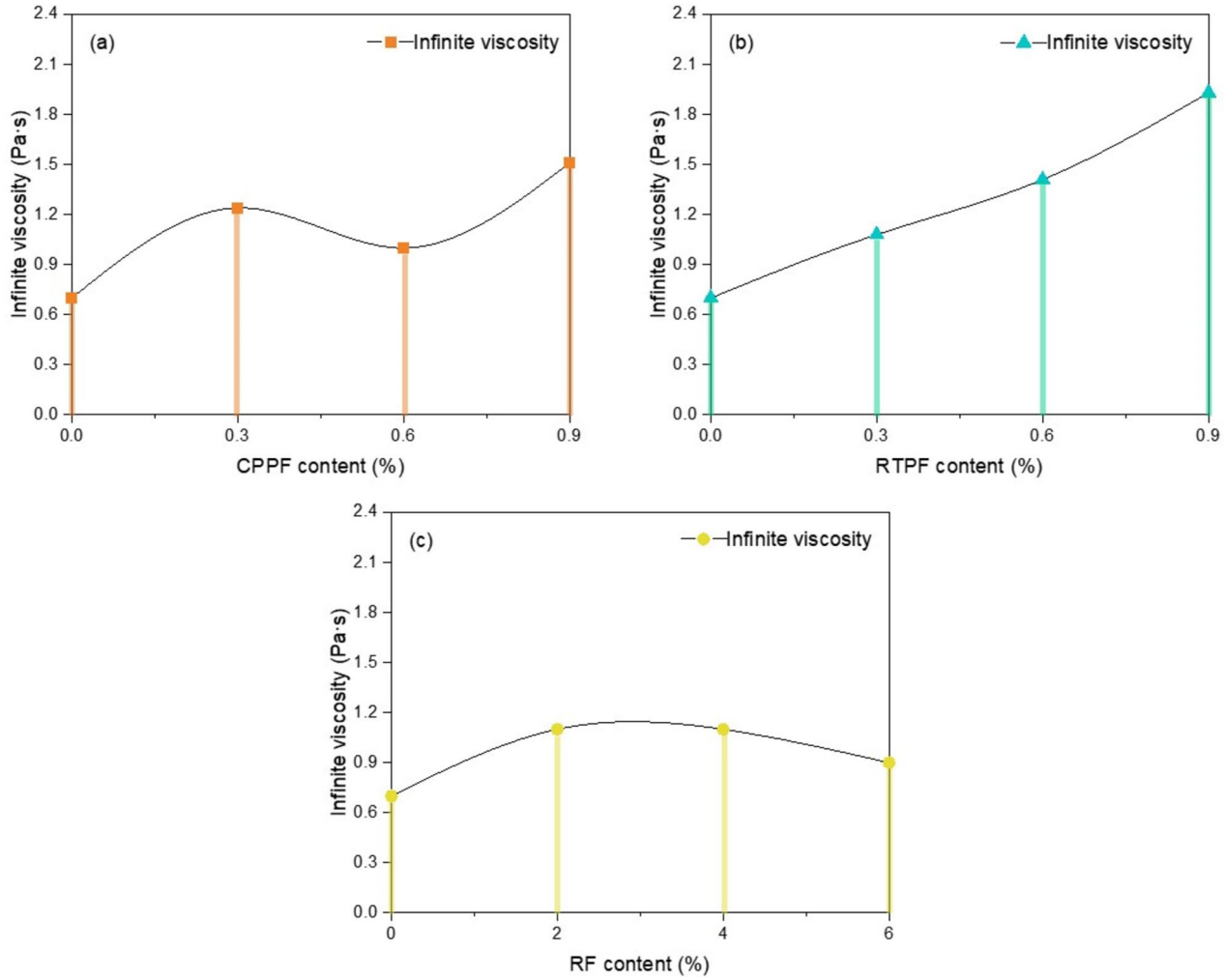

Figure 9. Infinite viscosity of CPB incorporated with (**a**) CPPF, (**b**) RTPF, and (**c**) RF.

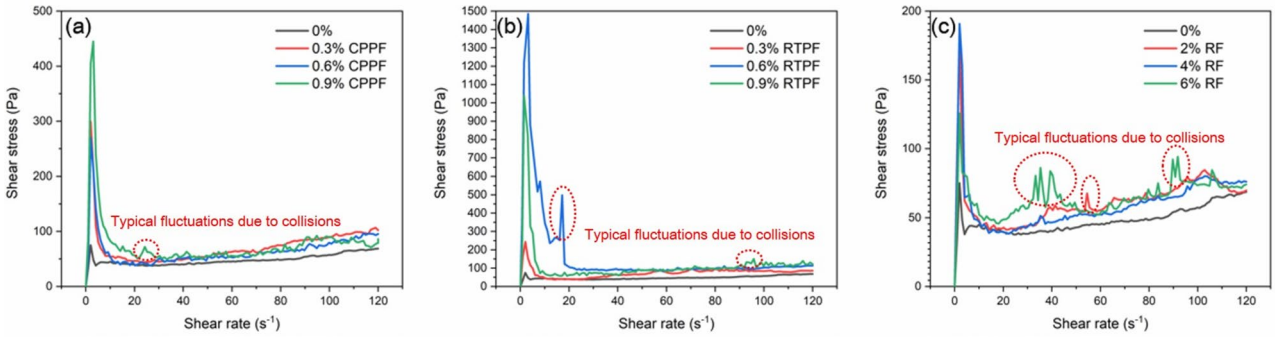

Figure 10. Flow curves of the CPB mixtures containing (**a**) CPPF, (**b**) RTPF, and (**c**) RF.

the rotation of the rotor. Although these fluctuations caused by the collision between the fibers and the blades increase fitting errors during rheological curve analysis, they do not significantly alter the overall trend of the curves. From a certain point within the shear rate range of approximately 10 to 20 s^{-1}, there is a steady increase in shear stress with an increasing shear rate.

The flow curves fitting was conducted using Bingham model as illustrated in Eq. (3) for providing the yield stress. It is noted that in the case of CPB being pumped through a pipeline, the shear rate is typically greater than 10 s^{-1}. Therefore, for engineering purposes, it is more relevant to focus on the rheological characteristics of CPB in a stable flow state. When fitting the flow curve of CPB, it is common practice to select the stable growth segment of the flow curve for fitting. Additionally, addressing the presence of fibers in the mixture, any interference fluctuations caused by fiber-blade collisions in flow curves are trimmed to ensure they do not avoid the fitting

results. Fitting results and Bingham parameters for CPB mixtures are shown in Table 5. The average R^2 value is 0.85, demonstrates a good fitting performance.

Effect of fibers on the plastic viscosity and yield shear stress of CPB mixtures

Figure 11 shows the plastic viscosity and yield shear stress of CPB mixtures in this study. Due to the incorporation of various polymer fibers, the relationship between the yield shear stress and plastic viscosity of the mixture no longer maintains a simple positive linear correlation. It can be observed from Fig. 11a that with the increase of CPPF content, the change in yield shear stress is not significant, only a mild increase occurs when the CPPF

CPB mixtures	Fitting results	Yield stress (Pa)	Plastic viscosity (Pa·s)	Coefficient of determination, R^2
0%	$\tau = 31.44 + 0.26\gamma$	31.44	0.26	0.87
0.3% CPPF	$\tau = 31.04 + 0.57\gamma$	31.04	0.57	0.93
0.6% CPPF	$\tau = 29.49 + 0.48\gamma$	29.49	0.48	0.91
0.9% CPPF	$\tau = 36.29 + 0.41\gamma$	36.29	0.41	0.73
0.3% RTPF	$\tau = 40.75 + 0.47\gamma$	40.75	0.47	0.74
0.6% RTPF	$\tau = 73.54 + 0.31\gamma$	73.54	0.31	0.80
0.9% RTPF	$\tau = 51.40 + 0.65\gamma$	51.40	0.65	0.87
2% RF	$\tau = 37.53 + 0.35\gamma$	37.53	0.35	0.86
4% RF	$\tau = 32.14 + 0.39\gamma$	32.14	0.39	0.95
6% RF	$\tau = 43.22 + 0.28\gamma$	43.22	0.28	0.83

Table 5. Fitting results and Bingham parameters for CPB mixtures.

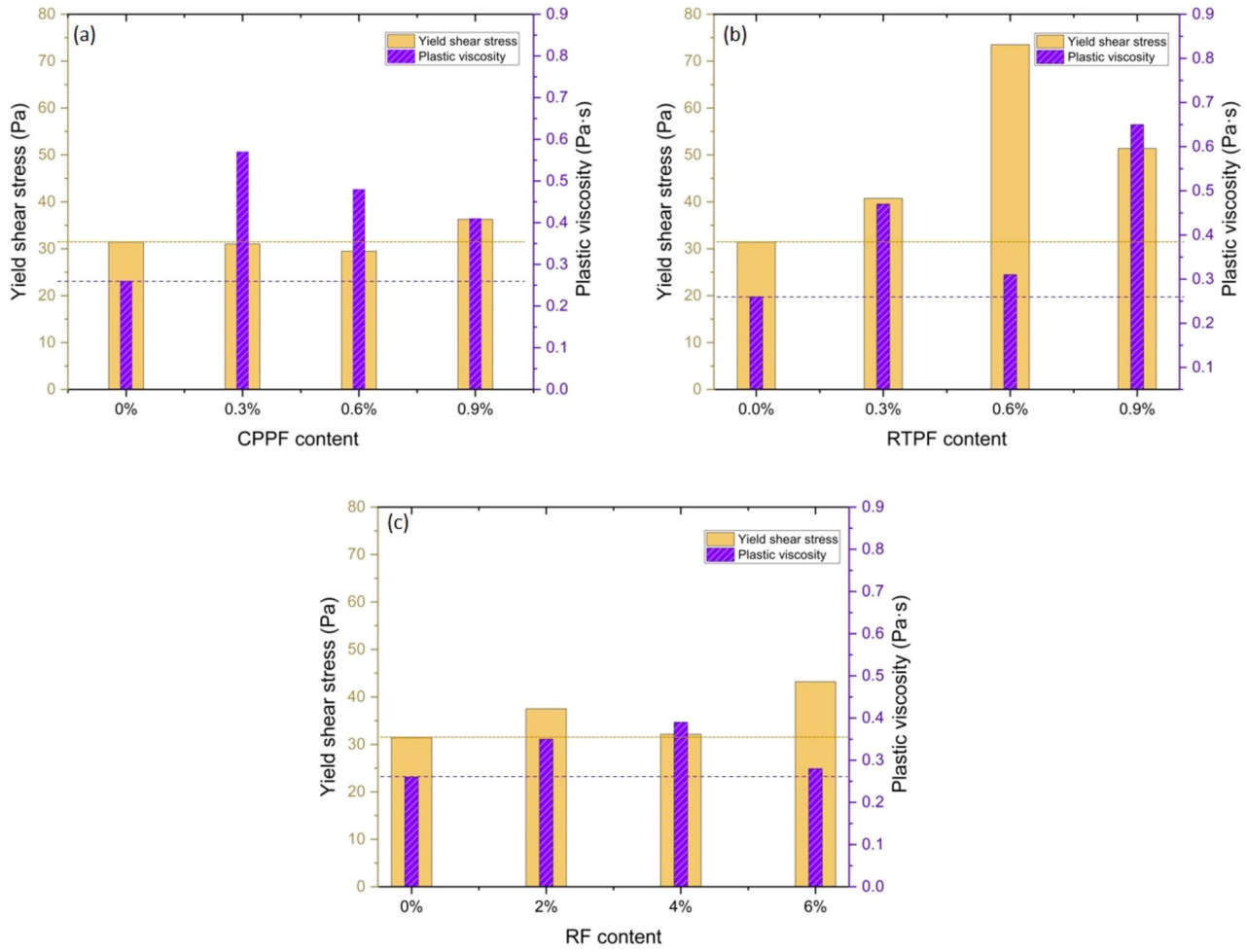

Figure 11. Effects of (**a**) CPPF, (**b**) RTPF, and (**c**) RTPF on the yield shear stress and plastic viscosity of CPB mixtures.

content reaches 0.9%. On the other hand, the plastic viscosity increases first and then decreases with the increase of CPPF content, reaching a peak at 0.3% fiber content. From Fig. 11b, it can be seen that the yield shear stress of CPB gradually increases with the increase of RTPF content, while the plastic viscosity first increases, then decreases at 0.6% fiber content, and then resumes an upward trend, reaching a peak at 0.9% fiber content. From Fig. 11c, it can be seen that with the increase of RF content, the yield shear stress oscillates, and the plastic viscosity increases first and then decreases, reaching a peak at 4% RF content.

It can be seen from the overview of rheometer test results obtained from the CPB incorporating polymer fibers that achieving identical rheological parameters to those of conventional CPB, devoid of any fiber inclusion, is unattainable. However, it can be noted that different polymer fibers exhibit distinct characteristics in their influence on the rheological properties of CPB. For CPPF and RF, the increase in content has a similar effect on the variation of the plastic viscosity of CPB, showing an initial increase followed by a decrease. Unlikely, the increase in RTPF content leads to oscillating increases in mixture plastic viscosity. As for the variation trend of yield shear stress, the addition of CPPF induces a marginal effect on the yield shear stress of CPB, while the introduction of RF results in a slightly more pronounced influence. A more distinct aspect is the incorporation of RTPF exhibits a substantially greater impact, notably enhancing the yield shear stress of CPB. This indicates that the observed variation trend in yield shear stress closely parallels the trend exhibited by slump tests despite the results of the 0.9% RTPF CPB. The decrease of yield shear stress when the fiber content reaches 0.9% may be attributed to the synergistic effect of rubber ash and fibers in RTPF. As can be seen from Fig. 12, the irregular shape and the rough surface of rubber ash particles possess a good shape retention ability together with the polyester fiber. When the RTPF content exceeds the critical level, its shape retention ability is greatly enhanced. Due to the approximate consistency between the stirring direction and the rheometer test rotation direction, the RTPF has maintained a shape that conforms to the flow direction, resulting in a decrease in yield stress. However, it is worth noting that at this point, the yield shear stress still remains at a relatively high value of 51.4 Pa.

Figure 13 summarizes the relationships between state structures and rheological properties of CPB incorporated with all types of polymer fibers investigated in this study. It is speculated that the effect of polymer fibers on plastic viscosity and yield shear stress is mainly due to the formation of a network structure, which restricts the particles in the mixture[42,43]. However, when the fiber content reaches a critical value, the high density of fibers leads to aggregation, reduced uniformity, and increased free water, resulting in a significant decrease in plastic viscosity. For CPB incorporated with RTPF, a significant decrease in plastic viscosity also occurs when fiber clusters entangle within the mixture. As the content of RTPF continues to increase, the rubber ash content reaches a critical level and locked with tailings particles by tangled fibers, substantially increasing the friction between particles and reducing the amount of free water, thereby increasing plastic viscosity. For CPPF and RF, the mechanism governing the effect of fiber content on yield stress is similar. When the content of CPPF and RF is relatively low, the spacing between fibers is large, resulting in minimal contact or collision opportunities. However, when the fiber content reaches a critical value, the mutual contact effect between fibers during flow increases significantly, thereby increasing the mixture yield shear stress. Considering the factor of size, CPPF is more susceptible to shape alteration than RF, leading to CPB incorporated with CPPF exhibiting a limited change in yield shear stress. While RTPF is softer than CPPF, its collaborative interaction with rubber ash particles gives it a higher capacity for shape retention, thereby showing a greater impact on the yield shear stress of CPB.

Through analysis and comparison of the impacts of RTPF, RF, and CPPF on rheometer test results of CPB, it can be concluded that (i) the impacts of polymer fibers on the plastic viscosity is more pronounced than that on the yield shear stress, but slump tests results may not fully realized; (ii) The macroscopic network framework of polymer fibers, molded by their geometric characteristics and frictional forces, plays a pivotal role in shaping the rearrange and flow states of CPB mixtures; (iii) the combined effects of rubber ash particles and polyester fibers in RTPF significantly influence rheological properties, particularly through their physical attributes, notably morphology, water absorption, and air permeability.

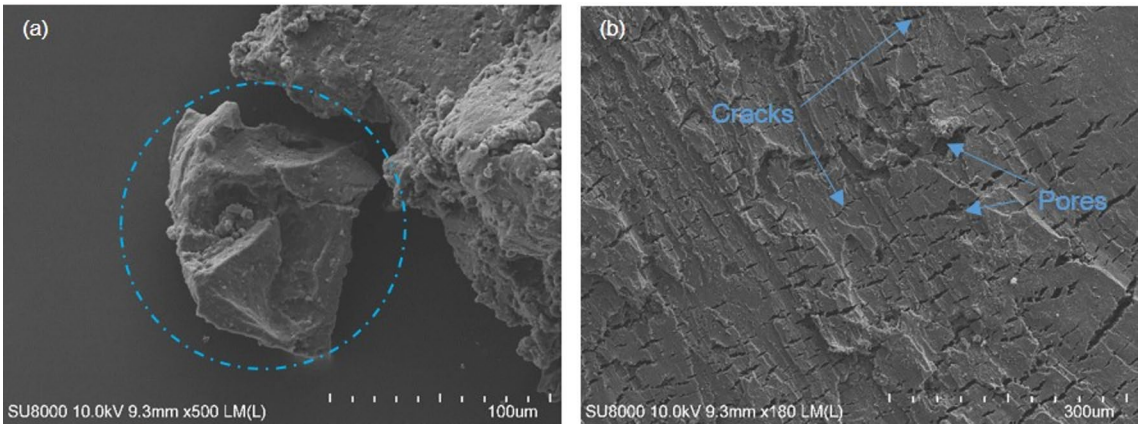

Figure 12. SEM images of rubber ash particles in RTPF: (**a**) a small particle exhibiting an irregular polyhedral structure, (**b**) a large particle featuring micro pores and surface cracks.

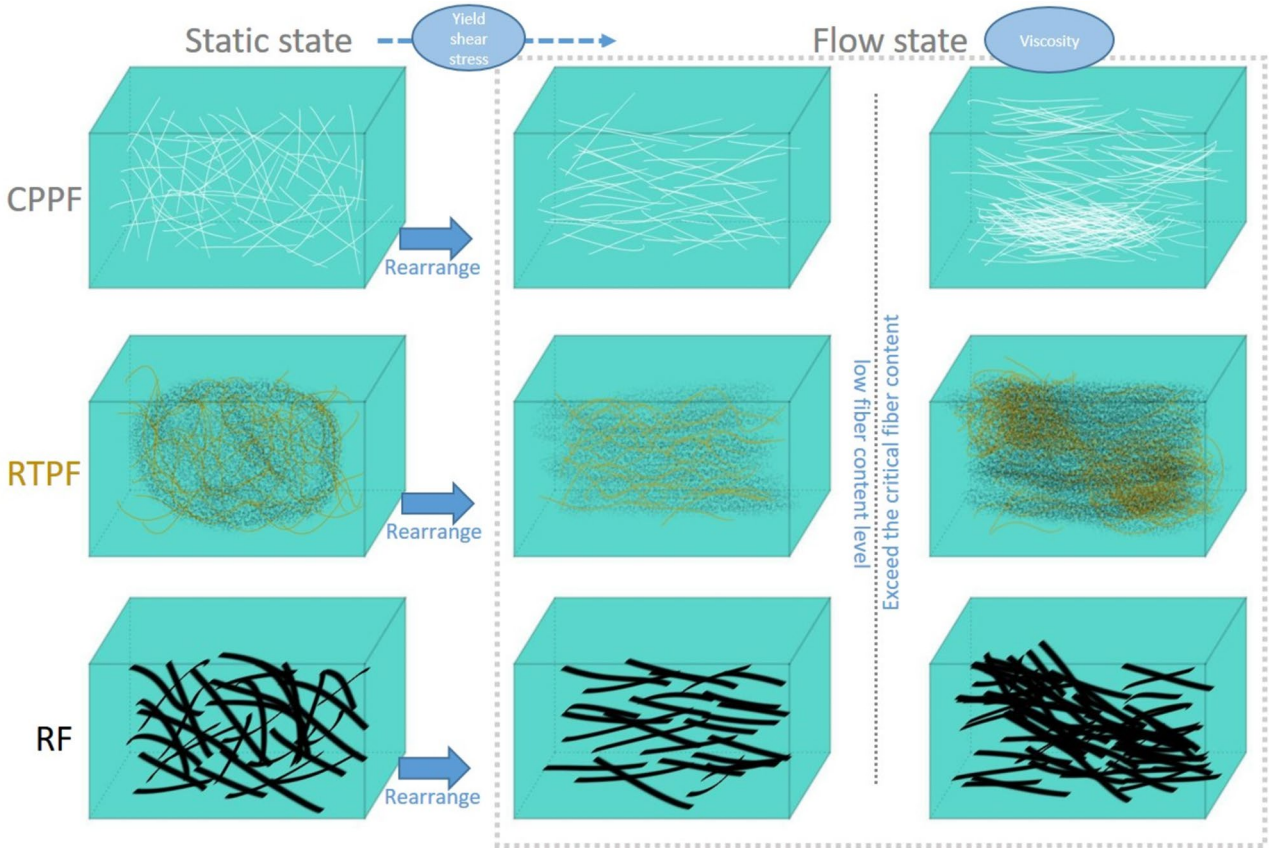

Figure 13. Schematic diagram of relationships between state structures and rheological properties of CPB incorporated with polymer fibers.

Conclusions

This study investigated the effect of polymer fibers addition in CPB on the rheological properties. On the basis of the investigation, following conclusions can be drawn:

- Addition of polymer fibers in CPB consistently leads to a continuous decrease in bulk density. However, the impact on slump varies with different types of polymer fibers. Among them, CPPF has a relatively minor effect on slump, RTPF causes a continuous decrease in slump, and RF has a minor impact on slump within a 4% content, but significantly reduces that beyond 4% content.
- CPB incorporating polymer fibers displays elevated apparent viscosity. As CPPF content rises, both the average apparent viscosity and infinite viscosity of CPB experience a fluctuating increase within a narrow range. As RF content increases, CPB's average apparent viscosity and infinite viscosity initially rise, then decline within a small interval. Conversely, the escalation of RTPF content induces the most significant variability in CPB's apparent viscosity, with infinite viscosity steadily increasing, while average apparent viscosity peaks before slightly decreasing.
- The collision between fibers and paddles induces fluctuations in the flow curve, necessitating trimming to mitigate adverse fitting effects, especially notable in CPB containing RF. The Bingham model exhibits excellent fitting capabilities for the flow curves of CPB containing polymer fibers with an average R^2 value of 0.85.
- Polymer fibers, particularly in CPPF and RF, have a stronger influence on the plastic viscosity of CPB compared to its yield stress, suggesting potential limitations of slump tests in fully capturing rheological properties.
- Macroscopic network structures of polymer fibers, shaped by geometry and friction, crucially affects the rearrangement and flow states of CPB mixtures. Rubber ash particles and polyester fibers in RTPF notably impact the yield shear stress of CPB, peaking at 0.6% RTPF content.

In practical engineering applications, adjusting transportation methods, design parameters, and additives is essential to accommodate the varying rheological properties influenced by different types and concentrations of polymer fibers. When utilizing RTPF for CPB reinforcement, it is crucial to focus on improving technical indicators related to viscosity, including energy consumption and pipeline wear during transport. However, effective methods to enhance rheological properties are not provided in this paper. Further investigations are required to determine the optimal methods for enhancing the rheological properties of CPB incorporated with recycled polymer fibers.

Data availability

Data available on request from the corresponding author (Z.Y.).

Received: 15 June 2024; Accepted: 25 July 2024
Published online: 01 August 2024

References

1. Beya, F. *et al.* Mine backfilling in the permafrost part I: Numerical prediction of thermal curing conditions within the cemented paste backfill matrix. *Minerals* **9**(3), 165 (2019).
2. Ma, D. *et al.* Effect of wetting–drying cycle on hydraulic and mechanical properties of cemented paste backfill of the recycled solid wastes. *Chemosphere* **282**, 131163 (2021).
3. Zhengzheng, C., Pengshuai, W., Zhenhua, L. & Feng, D. Migration mechanism of grouting slurry and permeability reduction in mining fractured rock mass. *Sci. Rep.* **14**(1), 3446 (2024).
4. Qi, C., Chen, Q., Fourie, A. & Zhang, Q. An intelligent modelling framework for mechanical properties of cemented paste backfill. *Miner. Eng.* **123**, 16–27 (2018).
5. Sheshpari, M. A review of underground mine backfilling methods with emphasis on cemented paste backfill. *Electron. J. Geotech. Eng.* **20**, 5183–5208 (2015).
6. Yi, X. W., Ma, G. W. & Fourie, A. Compressive behaviour of fibre-reinforced cemented paste backfill. *Geotext. Geomembr.* **43**(3), 207–215 (2015).
7. Simon-Lledo, E. *et al.* Ecology of a polymetallic nodule occurrence gradient: Implications for deep-sea mining. *Limnol Oceanogr* **64**(5), 1883–1894 (2019).
8. Ribeiro, M. C., Ferreira, R., Pereira, E. & Soares, J. Scientific, technical and legal challenges of deep sea mining. A vision for Portugal-conference report. *Marine Policy.* **1**(114), 103338 (2020).
9. Ziegler, M. *et al.* Mining-induced stress transfer and its relation to a Wm 19 seismic event in an ultra-deep south African gold mine. *Pure Appl. Geophys.* **172**(10), 2557–2570 (2015).
10. Furlan, J., Visintainer, R. & Sellgren, A. Centrifugal pump performance when handling highly non-Newtonian clays and tailings slurries. *Can. J. Chem. Eng.* **94**(6), 1108–1115 (2016).
11. Xue, Z., Gan, D., Zhang, Y. & Liu, Z. Rheological behavior of ultrafine-tailings cemented paste backfill in high-temperature mining conditions. *Constr. Build. Mater.* **30**(253), 119212 (2020).
12. Zhang, Q.-L. *et al.* Effects of temperatures and pH values on rheological properties of cemented paste backfill. *J. Central South Univ.* **28**(6), 1707–1723 (2021).
13. Xiapeng, P., Fall, M. & Haruna, S. Sulphate induced changes of rheological properties of cemented paste backfill. *Minerals Eng.* **1**(141), 105849 (2019).
14. Wu, A., Wang, Y. & Wang, H. Estimation model for yield stress of fresh uncemented thickened tailings: Coupled effects of true solid density, bulk density, and solid concentration. *Int. J. Mineral Process.* **143**, 117–124 (2015).
15. Ouattara, D., Yahia, A., Mbonimpa, M. & Belem, T. Effects of superplasticizer on rheological properties of cemented paste backfills. *Int. J. Mineral Process.* **161**, 28–40 (2017).
16. Yan, B., Ren, F., Cai, M. & Qiao, C. Influence of new hydrophobic agent on the mechanical properties of modified cemented paste backfill. *J. Mater. Res. Technol.* **8**(6), 5716–5727 (2019).
17. Xiao, B., Fall, M. & Roshani, A. Towards understanding the rheological properties of slag-cemented paste backfill. *Int. J. Mining Reclam. Environ* **35**(4), 268–290 (2020).
18. El Mahboub, K., Mbonimpa, M., Belem, T. & Maqsoud, A. Rheological characterization of cemented paste backfills containing superabsorbent polymers (SAPs). *Constr. Build. Mater.* **24**(317), 125863 (2022).
19. Guo, Z. *et al.* Effect of superplasticizer on rheology and thixotropy of superfine-tailings cemented paste backfill: Experiment and modelling. *Constr. Build. Mater.* **17**(316), 125693 (2022).
20. Vo, D. H. *et al.* Mechanical properties of concrete produced with alkali-activated slag-fly ash and recycled concrete aggregate and designed using the densified mixture design algorithm (DMDA) method: Effects of recycled aggregate content and alkaline solution. *Dev. Built Environ.* **1**(14), 100125 (2023).
21. Hamberg, R., Maurice, C. & Alakangas, L. The formation of unsaturated zones within cemented paste backfill mixtures-effects on the release of copper, nickel, and zinc. *Environ. Sci. Pollut. Res. Int.* **25**(21), 20809–20822 (2018).
22. Tuylu, S. Investigation of the effect of using different fly ash on the mechanical properties in cemented paste backfill. *J. Wuhan Univ. Technol. Mater. Sci. Ed.* **37**(4), 620–627 (2022).
23. Cao, S., Yilmaz, E. & Song, W. Fiber type effect on strength, toughness and microstructure of early age cemented tailings backfill. *Constr. Build. Mater.* **223**, 44–54 (2019).
24. Xue, G., Yilmaz, E., Song, W. & Yilmaz, E. Influence of fiber reinforcement on mechanical behavior and microstructural properties of cemented tailings backfill. *Constr. Build. Mater.* **213**, 275–285 (2019).
25. Zhao, K. *et al.* Study on energy dissipation and acoustic emission characteristics of fiber tailings cemented backfill with different ash-sand ratios. *Process Saf. Environ. Protect.* **174**, 983–996 (2023).
26. Chen, X. *et al.* Compressive behavior and microstructural properties of tailings polypropylene fibre-reinforced cemented paste backfill. *Constr. Build. Mater.* **190**, 211–221 (2018).
27. Chen, X., Shi, X., Zhou, J., Yu, Z. & Huang, P. Determination of mechanical, flowability, and microstructural properties of cemented tailings backfill containing rice straw. *Constr. Build. Mater.* **246**, 1–13 (2020).
28. Wang, Y., Yu, Z. & Wang, H. Experimental investigation on some performance of rubber fiber modified cemented paste backfill. *Constr. Build. Mater.* **271**, 1–13 (2021).
29. Yu, Z., Wang, Y. & Li, J. Performance investigation and cost–benefit analysis of recycled tire polymer fiber-reinforced cemented paste backfill. *Polymers.* **14**(4), 708 (2022).
30. He, W., Liu, L., Fang, Z., Gao, Y. & Sun, W. Effect of polypropylene fiber on properties of modified magnesium-coal-based solid waste backfill materials. *Constr. Build. Mater.* **2**(362), 129695 (2023).
31. Libos, I. L., Cui, L. & Liu, X. Effect of curing temperature on time-dependent shear behavior and properties of polypropylene fiber-reinforced cemented paste backfill. *Constr. Build. Mater.* **13**(311), 125302 (2021).
32. Jiang, H. *et al.* Effectiveness of alkali-activated slag as alternative binder on workability and early age compressive strength of cemented paste backfills. *Constr. Build. Mater.* **218**, 689–700 (2019).
33. Fall, M., Belem, T., Samb, S. & Benzaazoua, M. Experimental characterization of the stress–strain behaviour of cemented paste backfill in compression. *J. Mater. Sci.* **42**(11), 3914–3922 (2007).
34. Panchal, S., Deb, D. & Sreenivas, T. Variability in rheology of cemented paste backfill with hydration age, binder and superplasticizer dosages. *Adv. Powder Technol.* **29**(9), 2211–2220 (2018).
35. Festugato, L., Fourie, A. & Consoli, N. C. Cyclic shear response of fibre-reinforced cemented paste backfill. *Géotech. Lett.* **3**(1), 5–12 (2013).

36. Bekhiti, M., Trouzine, H. & Rabehi, M. Influence of waste tire rubber fibers on swelling behavior, unconfined compressive strength and ductility of cement stabilized bentonite clay soil. *Constr. Build. Mater.* **208**, 304–313 (2019).
37. ASTM, ASTM C 143, Standard test method for slump of hydraulic-cement concrete, ASTM International, West Conshohocken, 2010.
38. Niroshan, N., Sivakugan, N. & Veenstra, R. L. Flow characteristics of cemented paste backfill. *Geotech. Geol. Eng.* **36**(4), 2261–2272 (2018).
39. Haruna, S. & Fall, M. Time- and temperature-dependent rheological properties of cemented paste backfill that contains superplasticizer. *Powder Technol.* **360**, 731–740 (2020).
40. Xue, Z., Sun, H., Gan, D., Yan, Z. & Liu, Z. Wall slip behavior of cemented paste backfill slurry during pipeline based on noncontact experimental detection. *Int. J. Minerals Metall. Mater.* **30**(8), 1515–1523 (2023).
41. Stokes, J. R. & Telford, J. H. Measuring the yield behaviour of structured fluids. *J. Non-Newtonian Fluid Mech.* **124**(1–3), 137–146 (2004).
42. Thiébaud, F. & Gelin, J. C. Characterization of rheological behaviors of polypropylene/carbon nanotubes composites and modeling their flow in a twin-screw mixer. *Compos. Sci. Technol.* **70**(4), 647–656 (2010).
43. Albano, C., Camacho, N., Reyes, J., Feliu, J. L. & Hernández, M. Influence of scrap rubber addition to Portland I concrete composites: Destructive and non-destructive testing. *Compos. Struct.* **71**(3–4), 439–446 (2005).

Acknowledgements

The authors acknowledge the financial support from the National Natural Science Foundation Project of China (Grant No. 42071080 and No. 51674149).

Author contributions

Conceptualization, Z.Y.; data curation, Y.W.; writing—original draft preparation, W.K.; writing—review and editing, Z.Y. and Z.J.

Competing interests

The authors declare no competing interests.

Additional information

Correspondence and requests for materials should be addressed to Z.Y.

Reprints and permissions information is available at www.nature.com/reprints.

Publisher's note Springer Nature remains neutral with regard to jurisdictional claims in published maps and institutional affiliations.